DEVELOPMENTS IN CLARA ACCELERATOR DESIGN AND SIMULATIONS

S. Spampinati, University of Liverpool & The Cockcroft Institute, Warrington, Cheshire, U.K.
D. Angal-Kalinin, A. D. Brynes, D. Dunning, J. K. Jones, K. Marinov, J. W. McKenzie, B. L. Militsyn, N. R. Thompson, P. H. Williams, ASTeC, Daresbury Laboratory, Cheshire, U.K.
I. P. Martin, Diamond Light Source, Oxford, U.K.

Abstract

We present recent developments in the accelerator design of CLARA (Compact Linear Accelerator for Research and Applications), the proposed UK FEL test facility at Daresbury Laboratory. Updates on the electron beam simulations and code comparisons including wakefields are described. Simulations of the effects of geometric wakefields in the small-aperture FEL undulator are shown, as well as further simulations on potential FEL experiments using chirped beams. We also present the results of simulations on post-FEL diagnostics.

THE CLARA ACCELERATOR

CLARA (Compact Linear Accelerator for Research and Applications) is a proposed 250 MeV, 100-400 nm FEL test facility at Daresbury Laboratory [1]. The purpose of CLARA is to test and validate new FEL schemes in areas such as ultra-short pulse generation, temporal coherence and pulse-tailoring. The accelerator will comprise 4 S-Band, normal-conducting linacs with a medium-energy, variable bunch-compression scheme, feeding into a flexible arrangement of FEL modulators and radiators. For seeding the accelerator includes a pre-FEL dogleg where laser light can be introduced. The accelerator will be driven by a high rep-rate RF photocathode S-Band gun, operating in single bunch mode at up to 100 Hz, and with bunch charges up to 250 pC. Peak currents at the FEL are expected to be in the 500 A range, with increased currents possible through the use of velocity-bunching.

SIMULATION PLANS

Previous simulation work on the CLARA accelerator has relied on the ASTRA[2] code to simulate the injector up to the exit of the 1st linac (or the 2nd linac for velocity bunching schemes), feeding into *elegant* [3] for simulation of the rest of the machine. *Elegant* includes longitudinal space-charge forces, but not transverse space-charge. At the low energy of CLARA, the transverse beam dynamics are not adequately represented using *elegant* alone. There is an ongoing effort to remodel the design, up to the FEL section, in ASTRA. Simulation of the variable bunch compressor will still be performed in *elegant*, cross-checked with CSRTrack, so that CSR effects can be included. Design of the accelerator will also continue using *elegant*, due to the flexibility and rapid-prototyping inherent in the code. Additionally, wakefields from the 1st and 2nd injector linacs have not been previously included in the ASTRA simulations. For the velocity bunching scheme, these wakefields become more important due to the short bunch lengths involved.

INJECTOR WAKEFIELDS

To check the validity of the wakefield calculations in ASTRA, benchmarking was done using *elegant* for a simplified case, using the bunch properties given in Table 1, and tracking through 9 cells of an RF cavity.

Table 1: Beam Parameters for Wakefield Benchmarks

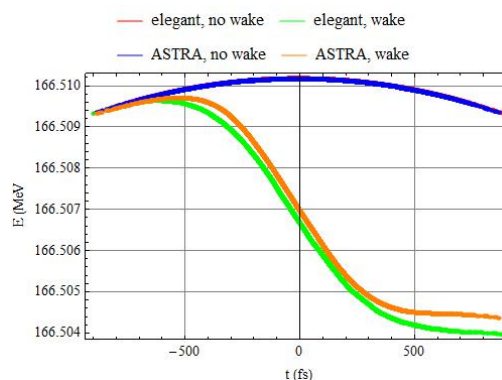|	
Initial energy (MeV)	160
Beam size (µm)	100
Bunch length (ps)	0.3 & 3
Transverse emittance (mm − mrad)	1
Bunch charge (pC)	100
Number of macro-particles	1000

Figure 1: Comparison of longitudinal phase space for a 300fs 100 pC bunch between ASTRA and ELEGANT.

The results for the 3 ps bunch show a negligible difference between the two codes. When the wakes are included for the 0.3 ps bunch (Fig. 1) there is a slight difference of a few hundred eV. The tail of the bunch is accelerated slightly more when simulated with ASTRA. However, these discrepancies have a very small effect on the final bunch properties of CLARA in the normal long bunch mode.

VACUUM VESSEL WAKEFIELDS

Simulation studies have been made of the effect of vacuum vessel wakefields on the performance of the FEL. This was done for two different operating modes, in order to confirm the previous estimates that a minimum undulator gap of 8 mm, corresponding to an internal vacuum vessel aperture of 6 mm, is acceptable.

Seeding Mode is intended for FEL schemes in which a seed laser modulates the electron bunch energy. For this mode the electron bunch, of charge 230 pC, is optimised to have a 250 fs flat-top region of constant 400 A peak current to accommodate up to ±100 fs jitter between electron bunch and seed laser. An elliptical vacuum vessel shape with small semi-axis b = 3 mm and large semi-axis a = 3b was used for the calculations of the wake potential.
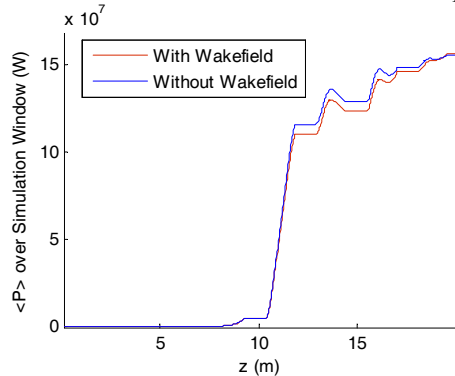

Figure 2: **Seeding Mode**: FEL power *vs* distance through undulator *z*, with and without wakefields included.

The material was copper at 273 K and the method for wake calculation given in [4]. The wake potential was imported into Genesis 1.3 to model the induced energy loss through the undulator. The simulation case was SASE at 100 nm output, with the same shot noise seed used for simulations with and without wakefields. The growth of the FEL power is shown for the two cases in Fig. 2. The effect of the wake potential is a reduction in output power of 8% with no change in the 14m saturation length. The wake potential was also artificially amplified by a factor of 10, giving a 25% reduction in output power compared to the case without wakefields.
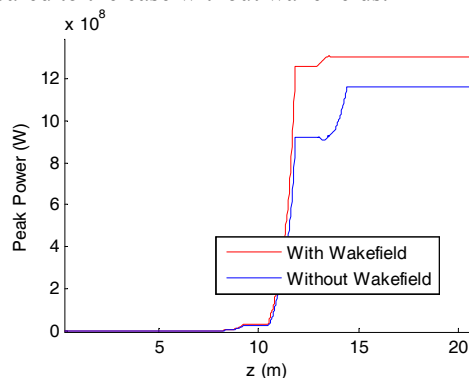

Figure 3: **Short Pulse Mode**: Peak power vs z, with and without wakefield included.

In Short Pulse mode a 100 pC bunch is compressed to a peak current of ~1500 A to obtain a bunch length of the order of the FEL cooperation length so the FEL can operate in weak super-radiant mode to generate a single SASE spike. The simulation results (Fig. 3) show the FEL peak power is enhanced by the presence of the wake potential. This can be understood by examining the longitudinal phase space of the electron bunch which has a strong intrinsic energy chirp which would normally

degrade the FEL interaction. The wake potential has the opposite sign and so acts to reduce the energy chirp.

CHIRP + TAPER SCHEMES

One of the seeded short-pulse FEL schemes that CLARA aims to demonstrate is the tapered undulator with energy-chirped electron beam, proposed by Saldin et al [5]. Preliminary studies in the λ_r = 266-400 nm range showed the facility design was well-suited, with the only issue likely to be generating a large enough energy modulation in the electron beam with the anticipated seed laser parameters (10 µJ, λ_L = 40-50 µm, 500 fs) .

Recent studies have focussed on combining two methods to increase the amplitude of energy modulation. The first step was to lower the beam energy from 228 MeV to 150 MeV, increasing the relative modulation amplitude without harming the ability to lase in the target wavelength range. The second step was to increase the peak current from 125 A to 400 A and to add a small chicane after the modulator. Tuning the R_{56} of the chicane allows the duration and gradient of the energy chirp to be controlled. As such, the part of the electron bunch with the correct chirp can be re-matched to the new FEL cooperation length, allowing a single SASE radiation spike to grow. Genesis 1.3 simulations show 'clean' FEL pulses of 280 MW peak power, 31 fs FWHM and excellent temporal coherence, as shown in Fig. 4.
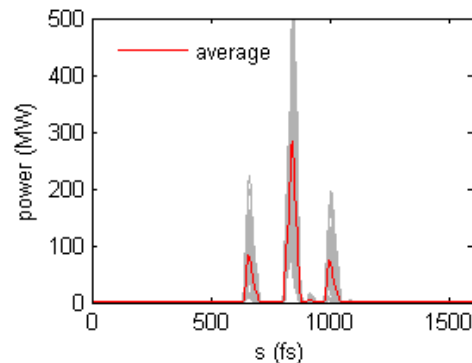

Figure 4: FEL pulse profile after 3 radiator modules over 50 shot-noise seeds for the tapered undulator short pulse scheme.

POST-FEL DIAGNOSTICS

Some advanced schemes depend on a manipulation of the electron beam properties with characteristic scales of several coherence lengths and shorter than the electron bunch [6,7,8]. To test mode locking and femto-slicing for the production of trains of short pulses [9,10,11] requires a 30 - 50 µm modulation of the beam energy, created via interaction with an IR laser beam in a short undulator.

The performances of these schemes depend on this energy modulation, so monitoring the longitudinal phase space is important. A transverse deflecting cavity (TDC) [13] installed in the last part of the FEL beam line allows the longitudinal beam distribution to be observed on a screen placed after the dipole leading to the beam dump.

Fig. 5 shows a possible layout of this diagnostic system, with a vertical TDC shown. This deflection maps the electron beam longitudinal coordinate to the vertical coordinate on a screen after the spectrometer dipole whilst the dipole converts energy to the horizontal coordinate.
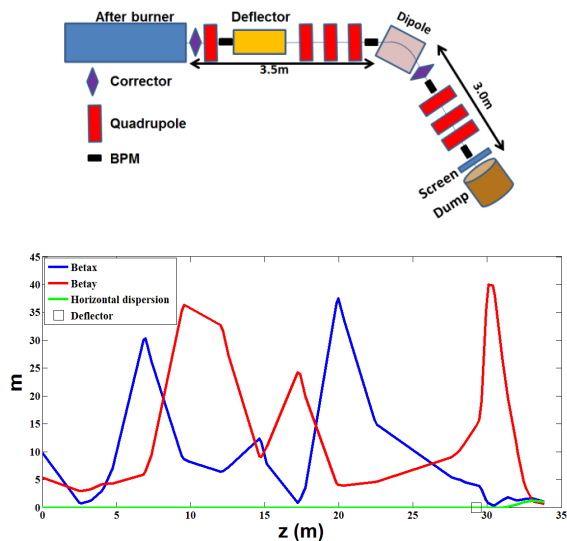

Figure 5: Layout of the phase space diagnostics (top) and potential optics solution (bottom) with transverse deflector and energy spectrometer.

The longitudinal resolution of the screen image can be written as:

$$\sigma_{L,r} = \frac{pc}{e_0 V k |\sin \Delta\Psi|} \sqrt{\frac{\varepsilon_n}{\gamma \beta_{yD}} + \frac{(\sigma_{screen})^2}{\beta_{yS} \beta_{yD}}} \qquad (1)$$

Here $k = 2\pi/\lambda$ and σ_{screen} is the screen resolution. V_0 is the deflecting voltage, $\beta_{y,D}$ an $\beta_{y,S}$ are vertical beta functions at the deflector and screen. $\Delta\Psi$ is the vertical phase advance between the deflector and screen, and $\lambda = 10.01$cm for a 2.998 GHz S-band cavity. The energy resolution of the spectrometer can be written as [13]:

$$\sigma_E = \sqrt{\frac{E^2}{\eta^2} \frac{\varepsilon_n \beta_x}{\gamma} + \frac{E^2}{\eta^2}(\sigma_{screen})^2 + (e_o V k)^2 \frac{\beta_y \varepsilon_n}{\gamma}} \qquad (2)$$

Here η is the horizontal dispersion at the screen. The first two terms represent the resolution of an energy spectrometer while the third term is the energy spread induced by the deflector [14].

The optimum phase advance between deflector and the screen is $\Delta\psi = 90^\circ$. Large values of V and $\beta_{y,D}$ give good longitudinal resolution but decrease the energy resolution via the induced energy spread. A small value of $\beta_{x,S}$ and a large value of η are required for good energy resolution. Fig. 5 also shows a possible optical solution from the modulator's exit to the screen. The radiators are at maximum gap and the intra-undulator quadrupoles are used along with those shown in Fig.5 to give the required resolution. The optics shown is for a beam energy of 150 MeV and gives a longitudinal resolution of 6.5 μm and an energy resolution of 50 keV with a deflecting voltage of 5 MV, calculated using Eq. 1 & 2. The vertical

rms beam size on the screen is 1.8 mm. With a beam energy of 250 MeV, similar resolution can be achieved with similar optics but with a deflecting voltage of 7.5 MV. Simulations have been performed with the code *elegant* to test the analytic results. An example of the simulated phase space imaged on the screen is shown in Fig. 6 - this is from a beam modulated with a few (FWHM 500 fs) cycle 50 μm laser with a peak power of 30 MW. Two million particles were used in this simulation. The screen image clearly shows energy modulations as predicted by the analytical equations above.
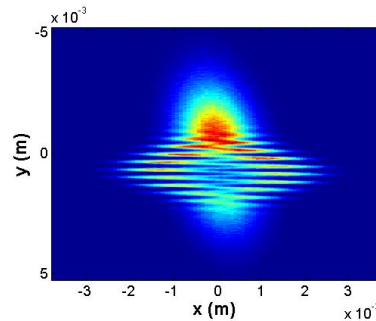

Figure 6: Beam imaged on the spectrometer screen.

CONCLUSION

Updates on CLARA beam simulation work presented here will enable a more accurate and consistent model for the future design work, and the more systematic inclusion of accelerating structure wakefields should provide improved confidence in the future results. Updates on the FEL side of the machine have concentrated on the undulator wakefields, where we have concluded that a minimum gap of 8mm is acceptable - for seeded mode bunches the wake potential has only a small detrimental impact on the FEL power and for low charge, short pulse operation, the wake potential reduces the energy chirp and improves the FEL performance. Work on several potential FEL seeding schemes has also continued with new work demonstrating the applicability of the Chirp + Taper schemes on CLARA shown here. Finally we have presented new results on the viability of post-FEL diagnostics on CLARA, and their expected performance.

REFERENCES

[1] J A Clarke et al 2014 JINST 9 T05001.

[2] M. Borland, "elegant: A Flexible SDDS-compliant Code for Accelerator Simulation", APS LS-287, (2000).

[3] K. Flottmann, "Astra - A Space Charge Tracking Algorithm", http://www.desy.de/~mpyflo/

[4] A. Lutman, R. Vescovo and P. Craievich, Phys. Rev. STAB 11, 074401, 2008.

[5] E.L. Saldin et al., Phys. Rev. ST. Accel. Beams 9, 050702, (2006).

[6] A.A. Zholents, W.M. Fawley, Phys. Rev, Lett. 92, 224801 (2004).

[7] E. Kur, D.J. Dunning, B.W.J. McNeil, J. Wurtele and A.A. Zholents, New J. Phys. 13 063012 (2011).

[8] D.J. Dunning, B.W.J. McNeil and N.R. Thompson, Phys. Rev. Lett. 110, 104801 (2013).

[9] E.L. Saldin, E.A. Schneidmiller and M.V. Yurkov, Phys.Rev. ST Accel. Beams 9, 050702 (2006).

[10] N.R. Thompson and B.W.J. McNeil, Phys. Rev. Lett. 100,203901 (2008).

[11] L. Giannessi et al., Phys. Rev. Lett. 106,144801 (2011).

[12] G. A. Loew, O.H. Altenmueller, SLAC, PUB-135. Aug. 1965.

[13] Y. Ding et al., Proceedings of IPAC conference 2013, Shangai, China.

[14] M. Cornacchia and P. Emma, Phys. Rev. ST Accel. Beams 5, 084001 (2002).